Protein Science (1999), *8*:722–730. Cambridge University Press. Printed in the USA.

Dissection of the structural and functional role of a conserved hydration site in RNase T1

ULRIKE LANGHORST,[1] REMY LORIS,[1] VLADIMIR P. DENISOV,[3] JAN DOUMEN,[1] PATRICE ROOSE,[2] DOMINIQUE MAES,[1] BERTIL HALLE,[3] AND JAN STEYAERT[1]

[1]Dienst Ultrastructuur, Vlaams Interuniversitair instituut voor Biotechnologie, Vrije Universiteit Brussel, Paardenstraat 65, B-1640 Sint-Genesius-Rode, Belgium
[2]Dienst Magnetische Resonantie, Vrije Universiteit Brussel, Pleinlaan 2, 1050 Brussel, Belgium
[3]Condensed Matter Magnetic Resonance Group, Department of Chemistry, Lund University, P.O. Box 124, S-22100 Lund, Sweden

(RECEIVED October 26, 1998; ACCEPTED December 8, 1998)

Abstract

The reoccurrence of water molecules in crystal structures of RNase T1 was investigated. Five waters were found to be invariant in RNase T1 as well as in six other related fungal RNases. The structural, dynamical, and functional characteristics of one of these conserved hydration sites (WAT1) were analyzed by protein engineering, X-ray crystallography, and ^{17}O and ^{2}H nuclear magnetic relaxation dispersion (NMRD). The position of WAT1 and its surrounding hydrogen bond network are unaffected by deletions of two neighboring side chains. In the mutant Thr93Gln, the Gln93Nϵ2 nitrogen replaces WAT1 and participates in a similar hydrogen bond network involving Cys6, Asn9, Asp76, and Thr91. The ability of WAT1 to form four hydrogen bonds may explain why evolution has preserved a water molecule, rather than a side-chain atom, at the center of this intricate hydrogen bond network. Comparison of the ^{17}O NMRD profiles from wild-type and Thr93Gln RNase T1 yield a mean residence time of 7 ns at 27 °C and an orientational order parameter of 0.45. The effects of mutations around WAT1 on the kinetic parameters of RNase T1 are small but significant and probably relate to the dynamics of the active site.

Keywords: conserved water; hydrogen bond network; NMRD; protein hydration; residence time; RNase T1

The structure and function of proteins and other biological macromolecules depend on their interaction with the surrounding aqueous solvent via the hydrophobic effect, dielectric screening, and specific hydrogen bonds. Most globular proteins contain a few water molecules buried in cavities. Such internal water molecules heal packing defects and extend the intramolecular hydrogen bond framework, thus contributing importantly to protein structure and stability, and are sometimes directly involved in enzyme catalysis (Meyer, 1992). Because they are conserved among homologous proteins to the same extent as amino acid residues (Baker, 1995), internal water molecules are clearly an integral part of the protein structure. The residence times of these internal water molecules are typically in the range 10^{-8}–10^{-6} s at ambient temperature (Denisov & Halle, 1996), but may be as long as 200 μs at 27 °C (Denisov et al., 1996).

The several hundred water molecules that make contact with the surface of a small protein are considered much more mobile (Denisov & Halle, 1996), and the relationship between hydration in solution and the water sites that are found in macromolecular crystal structures is poorly understood. In the present study, we analyze the reoccurrence of water molecules in the different crystal structures of RNase T1 and the related RNases F1, Ms, Ap, Pb, Th, and U2. Based on the results of this comparative study, a single water molecule is chosen (referred to as WAT1), of which the structural, dynamical, and functional properties are investigated using site-directed mutagenesis and X-ray crystallography. From the analysis of NMRD profiles, the mean residence time and orientational order parameter of WAT1 are calculated. This is the first determination of these quantities for an individual water molecule at the surface of a protein.

Reprint requests to: Remy Loris, Dienst Ultrastructuur, Vlaams Interuniversitair instituut voor Biotechnologie, Vrije Universiteit Brussel, Paardenstraat 65, B-1640 Sint-Genesius-Rode, Belgium; e-mail: reloris@vub.ac.be.

Results and discussion

Water molecules as recurring structural motifs in fungal ribonucleases

In a pioneering study, Malin and coworkers (Malin et al., 1991) compared the water molecules identified in four isomorphous RNase T1-inhibitor complexes. In the present study, we compared the crystallographically determined water molecules of Protein Data Bank (PDB) entry 1rga (our reference structure—Zegers et al., 1994) with all other crystal structures of RNase T1 and the closely related ribonucleases. At present, 10 structures are available in the Brookhaven database that are isomorphous with 1rga (PDB entries

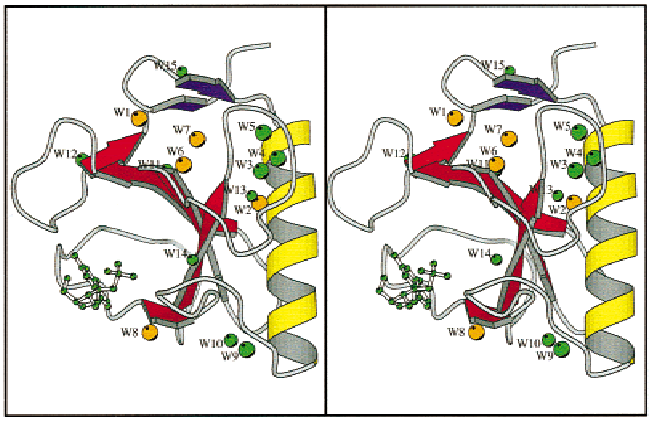

Fig. 1. Stereoview of a ribbon diagram of RNase T1 illustrating the reoccurrence of waters in different crystal structures of RNase T1 as well as the related RNases Ap, Ms, F1, Pb, Th, and U2. Water molecules present in all of these RNases are shown as orange spheres. Those waters conserved in different crystal environments of RNases T1 are shown as green spheres. The size of the spheres representing the water molecules relates to the number of RNase T1 packing environments in which the water is present (large sphere 10/10 packing environments, medium 9/10, and small 8/10).

1rnt, 2rnt, 3rnt, 6rnt, 7rnt, 8rnt, 9rnt, 2aae, 1rgk, and 1rgl). These 10 structures have 28 waters in common with 1rga, while another nine are present in all but one of these 10 structures. These 37 waters form a sizable fraction of the total number of waters present in each of these structures (between 75 and 142).

When different crystal packing environments of RNase T1 are compared, however, the number of structurally conserved water molecules reduces drastically. Only six waters of 1rga are completely conserved in the nine other crystal packing environments available (derived from six crystal forms: 1gsp, 1det, 1rn1, 1rn4, 4rnt, and 1lra). Another five are present in all but one packing environments, and another five in all but two (Fig. 1). These waters will be referred to as WAT1 to WAT16 in the following sections of the current paper. These highly conserved water molecules are generally not involved in crystal lattice contacts, have mostly low *B*-values (6.6–33.1 Å^2), and are located in crevices, shielded from bulk solvent (accessible surface area 0.9–37.8 Å^2 compared to 98.5 Å^2 for a completely isolated water molecule). They are typically hydrogen bonded to main-chain nitrogen and oxygen. Most of them occur isolated, with the exception of a chain formed by WAT2–WAT5. Also WAT6 and WAT7 hydrogen bond to each other, and are located fairly close to the chain WAT2–WAT5, interacting with the same hairpin loop. Mainly due to the confounding influence of rapidly exchanging OH and NH protons, WAT2, WAT3, and WAT4 were the only potentially long-lived water molecules that were unambiguously identified in a recent NOE study of RNase T1 hydration (Pfeiffer et al., 1998). Information about the residence time was obtained only for WAT4, for which the positive NOESY cross-peak intensity suggested $\tau_W > 300$ ps. In the same NOE study, the absence of a NOESY cross peak of WAT6 with the Ile61 γ-methyl protons was taken as evidence for a residence time of about 300 ps (where the NOESY cross-peak intensity passes through zero for a rigidly bound water molecule). Considering the rather long distance (5.4 Å between Ile61 γ-C and W6 O), however, it is doubtful whether a cross peak would have been observed even for a longer residence time.

Next, we investigated whether any of these conserved, crystal lattice-independent water molecules are present in the related ribonucleases F1, Ms, Ap, Pb, Th, and U2. Five waters (WAT1, WAT2, WAT6, WAT7, and WAT8) are present in each of these structures (Fig. 1). Not unexpectedly, these are the least accessible waters in 1rga (accessible surface area 0.9–15.6 Å^2). With the exception of WAT8, they have the lowest temperature factors (6.6–12.2 Å^2). In analogy to amino acids that are conserved during evolution, it is tempting to speculate that these waters play an important role in the structure, function, stability, or folding of the protein.

Geometry of the WAT1 hydration site

It is not within the scope of the current paper to describe each of the waters identified in the previous section in detail. Rather, we will focus on a single water molecule, WAT1, of which we investigated the physicochemical properties in detail. Water molecule WAT1 differs from all other conserved waters in RNase T1 because most of its hydrogen bonding partners are side-chain atoms. It is therefore the only water molecule in RNase T1 with a possible structural or functional role (it is conserved among different ribonucleases) that can be studied by conventional protein engineering techniques. We determined a series of isomorphous crystal structures of mutants of RNase T1 intended to affect the binding of WAT1. All these crystal structures are isomorphous, and belong to a novel crystal form of space group $P2_12_12_1$ with four molecules in the asymmetric unit (see Materials and methods; Table 1). Therefore, we also determined the structure of wild-type RNase T1 in this new crystal form. We will use this structure as a reference in the remainder of the paper.

The overall structures of the wild-type and mutant RNase T1 molecules are very similar to those previously found in other crystal forms of RNase T1. WAT1 is present in each of the four molecules in the asymmetric unit of wild-type RNase T1, located in a cleft (Fig. 2A) formed by the three hairpin loops L5 (Cys6–Asn9), L6 (Ile61–Asp76), and L8 (Thr91–Phe100). The average accessible surface area of WAT1 is 6.3 ± 0.3 Å^2. Among the four molecules in the asymmetric unit, the variations of the relevant Y···O(W) distances (Table 2) and Y···O(W)···Y angles (Table 3) in this hydration site are small. The average *B*-factor of WAT1 is similar to those of Cys6(O), Asn9(Nδ2), Asp76(Oδ1), Thr91(Oγ1), and Thr93(Oγ1) and to the overall *B*-factor of the whole protein (Table 4).

WAT1 forms three short hydrogen bonds (2.7–3.0 Å) to side-chain oxygens of Asp76 and Thr93 and the main-chain C=O of Cys6 (Table 2; Fig. 3A). The side-chain atoms Thr91(Oγ1) and Asn9(Nδ2) are located at 3.4 ± 0.1 Å and 3.5 ± 0.1 Å from WAT1, respectively. The pK_a of Asp76 in the folded enzyme is very low (p$K_a < 2$; A. Giletto & N. Pace, pers. obs.), indicating Asp76 to be deprotonated at our crystallization conditions. The orientation of the Asn9 amide is such that the contact between the Asn9(Nδ2) and WAT1 is probably of van der Waals type. Structurally, the closest donor/acceptor sites Cys6(O), Asp76(Oδ1), and Thr93(Oγ1) occupy three corners of an almost perfect tetrahedron with WAT1 in the center. The Cys6(O)–WAT1–Asp76(Oδ1), Cys6(O)–WAT1–Thr93(Oγ1), and Asp76(Oδ1)–WAT1–Thr93(Oγ1) angles are close to 109.4° (Table 3). The fourth coordination points to bulk water. Although no water molecule is visible in the electron density map, a positional disordered solvent molecule may occupy this fourth position. The order parameter derived from NMRD experiments

Table 1. *Crystallographic data*

	Wild-type	Asn9Ala	Thr93Ala	Thr93Gln
Crystallization conditions	10 mg/mL protein 25 mM NaAc, pH 4.2 2.8 mM 2′ GMP 6.25 mM $CaCl_2$ 47.5% MPD[a]	10 mg/mL protein 25 mM NaAc, pH 4.2 2.8 mM 2′ GMP 6.25 mM $CaCl_2$ 45% MPD[a]	10 mg/mL protein 25 mM NaAc, pH 4.2 2.8 mM 2′ GMP 6.25 mM $CaCl_2$ 42.5% MPD[a]	10 mg/mL protein 25 mM NaAc, pH 4.2 2.8 mM 2′ GMP 6.25 mM $CaCl_2$ 42.5% MPD[a]
Space group	$P2_12_12_1$	$P2_12_12_1$	$P2_12_12_1$	$P2_12_12_1$
Unit cell				
a (Å)	59.34	59.37	59.32	59.36
b (Å)	60.59	60.56	60.31	60.55
c (Å)	100.93	101.17	101.03	100.82
Number of molecules per asymmetric unit	4	4	4	4
Number of unique reflections	28,421	28,731	21,739	26,956
Number of measured reflections	138,761	205,057	64,065	64,065
Completeness	96.7%	98.0%	92.8%	98.8%
Resolution (Å)	20.0–1.90	15.0–1.90	15.0–2.05	15.0–1.95
R_{merge}	0.061	0.124	0.065	0.140
$I/\Sigma I$	15.9	13.3	11.9	17.9
R-value	0.177	0.168	0.190	0.167
R_{free}-value	0.219	0.209	0.234	0.213
Ramachandran				
Most favored	91.0%	91.6%	90.7%	91.9%
Additionally allowed	8.7%	8.1%	9.0%	8.1%
Generous	0.3%	0.3%	0.3%	0.0%
Disallowed	0.0%	0.0%	0.0%	0.0%
RMS				
Bond lengths (Å)	0.006	0.006	0.007	0.006
Bond angles (°)	1.469	1.265	1.452	1.505
Dihedral angles (°)	24.653	25.183	24.820	25.137
Improper angles (°)	1.037	1.019	1.067	1.071
Number of water molecules per asymmetric unit	242	212	219	229

[a]MPD, 2-methyl-2,4-pentanediol.

(see below) nevertheless shows that WAT1 is not rigidly bound to the protein but has substantial rotational freedom, allowing other hydrogen bond geometries involving Thr91 also to occur.

The structural integrity of the hydrogen bond network

We analyzed the structural integrity of the hydrogen bond network involving WAT1 by protein engineering. For this purpose, we determined the isomorphous crystal structures of the Asn9Ala, Thr93Ala, and Thr93Gln mutants that were designed to disrupt a part of this network (Table 1; Fig. 3B–D).

These three mutations hardly perturb the local structure of the protein. In the structures of wild-type, Asn9Ala, and Thr93Ala RNase T1, the oxygen atom of WAT1 is conserved at the same location in the 12 independently refined molecules. In the four independent molecules present in the asymmetric unit of the crystals of the Asn9Ala mutant, the side chain of Asn9 is replaced by a single water molecule (WAT A in Fig. 3B). The oxygen atom of WAT A in the mutant structure is at a distance of 1.4 ± 0.2 Å from the Nδ2 atom in Asn9 in the wild-type structure. WAT A is hydrogen bonded to another water molecule (WAT B), which in turn forms a hydrogen bond with the backbone NH of Ala75. In contrast, the Thr93Ala mutant does not accommodate any additional water molecules near the WAT1 hydration site (Fig. 3C).

In the crystal structure of the Thr93Gln mutant, we find that the Nϵ2 nitrogen of Gln93 structurally replaces WAT1 (Fig. 3D). The orientation of the Gln93 amide, with the nitrogen replacing WAT1 rather than the oxygen, was chosen because the closest hydrogen bonding partners of Gln93(Nϵ2), i.e., Asp76(Oδ1) and Cys6(O), are both acceptors.

Table 2. *Interatomic distances (Å) between WAT1/Nϵ2 and the surrounding O and N atoms*

	Wild-type[a]	Asn9Ala[a]	Thr93Ala[a]	Thr93Gln[a]
Cys6(O)···WAT1	3.0 ± 0.1	2.9 ± 0.1	3.1 ± 0.1	—
Thr93(Oγ1)···WAT1	2.7 ± 0.1	2.7 ± 0.1	—	—
Asp76(Oδ1)···WAT1	2.8 ± 0.1	2.8 ± 0.1	2.8 ± 0.2	—
Thr91(Oγ1)···WAT1	3.4 ± 0.1	3.4 ± 0.1	3.6 ± 0.1	—
Asn9(Nδ2)···WAT1	3.5 ± 0.1	—	3.2 ± 0.1	—
Cys6(O)···Gln93(Nϵ2)	—	—	—	3.0 ± 0.1
Asp76(Oδ1)···Gln93(Nϵ2)	—	—	—	2.9 ± 0.1
Thr91(Oγ1)···Gln93(Nϵ2)	—	—	—	3.6 ± 0.2
Asn9(Nδ2)···Gln93(Nϵ2)	—	—	—	3.5 ± 0.2

[a]Average value calculated from four molecules in one asymmetric unit.

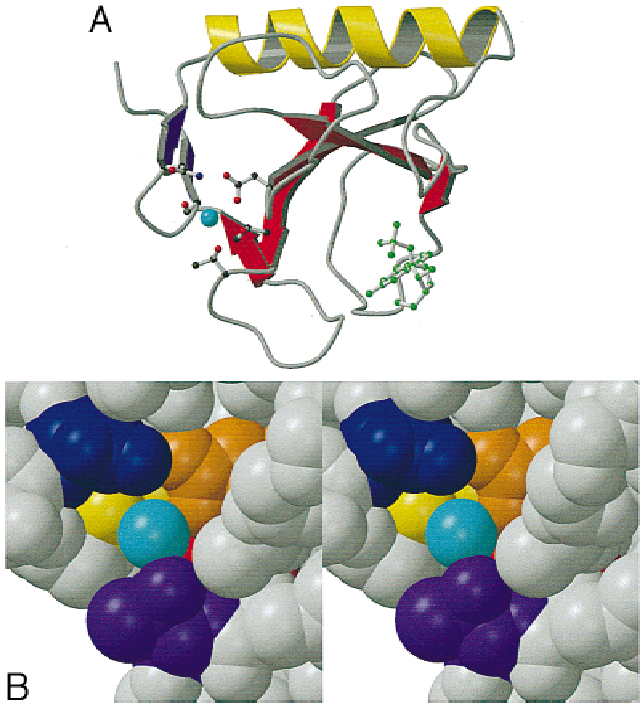

Fig. 2. A: Ribbon drawing showing the overall structure of RNase T1 and the location of WAT1. All residues involved in the hydration site (Asn9, Cys6, Asp76, Thr91, and Thr93) and the competitive inhibitor 2′ GMP (green) are shown in ball-and-stick representation. WAT1 is represented as a light blue sphere. **B:** Close-up of the hydration site. A space-filling model of RNase T1 is shown with the relevant residues colored: Asn9, dark blue; Cys6, yellow; Asp76, orange; Thr91, red; Thr93, purple; and WAT1, light blue. The orientation is identical to Figure 1A. All figures were drawn using BOBSCRIPT (Esnouf, 1997).

The network of intermolecular hydrogen bonds is invariant to these three side-chain deletions/substitutions. Tables 2 and 3 show that the corresponding interatomic distances and Y···O(W)···Y angles are very similar in all the investigated variants. These structural data indicate that WAT1 is at a fixed position, invariant to deletions of the Asn9 or Thr93 side chains. The interactions with WAT1 thus appear to be mutually independent. The position of WAT1 seems to be optimal to interact with each partner individually; each interacting partner predefines the same position of WAT1. We conclude that the different secondary structure elements fold together to accommodate a dynamic water molecule in a lock and key type fashion.

Residence time and orientational order of WAT1 in wild-type RNase T1

The ^{17}O relaxation dispersions from wild-type RNase T1 and the Thr93Gln mutant are shown in Figure 4A. The curves resulted from the usual three-parameter fit with a Lorentzian spectral density function (Denisov & Halle, 1996; Halle et al., 1998). The dispersion is due to a small number N_β of water molecules with residence times τ_w in the range 10^{-9}–10^{-6} s. Previous ^{17}O NMRD studies of numerous proteins have established that such long-lived water molecules are buried in internal cavities, coordinated to protein-bound divalent metal ions, or located in surface pockets with restricted accessibility to external solvent and with multiple hydrogen bonds to the protein (Denisov & Halle, 1996, 1998). The dispersion frequency yields a correlation time τ_β that is related to the water residence time and the rotational correlation time τ_R of the protein: $1/\tau_\beta = 1/\tau_R + 1/\tau_w$. The magnitude (or integral) of the dispersion step yields the product $N_\beta S^2$ of the number N_β of long-lived water molecules and their mean-square orientational order parameter S^2. The high-frequency relaxation enhancement (above the bulk water relaxation rate) yields the third parameter $N_\alpha \rho$, i.e., the product of the number N_α of water molecules in contact with the protein surface and the relative dynamic retardation ρ (relative to bulk water) averaged over these water molecules. The parameter values resulting from the fits in Figure 4 and from other fits to be discussed are collected in Table 5.

Because the structures of wild-type and Thr93Gln RNase T1 are virtually identical, except for the replacement of WAT1 by the side chain of Gln93 in the mutant, the parameters τ_β and $N_\alpha \rho$ are expected to be the same for the two proteins. This is indeed found to be the case (cf. Table 5). The correlation time, $\tau_\beta = 6.5 \pm 0.3$ ns, is close to the tumbling time, $\tau_R = 5.3$ ns (corrected to our

Table 3. *Analysis of all the Y···O(W)···Y angles (α) of the hydration site*[a]

Y···O(W)···Y					α (°)			
Y		O(W)		Y	Wild-type[b]	Asn9Ala[b]	Thr93Ala[b]	Thr93Gln[b]
Asn9(Nδ2)	–	WAT1/Nε2	–	Thr91(Oγ1)	135.5 ± 3.7	—	137.0 ± 6.0	131.6 ± 3.7
Asn9(Nδ2)	–	WAT1/Nε2	–	Asp76(Oδ1)	84.0 ± 3.0	—	90.3 ± 4.5	85.0 ± 1.9
Asn9(Nδ2)	–	WAT1/Nε2	–	Thr/Gln93(Oγ1/Cδ)	151.9 ± 12.4	—	—	131.7 ± 7.9
Asn9(Nδ2)	–	WAT1/Nε2	–	Cys6(O)	79.9 ± 3.7	—	81.8 ± 5.2	83.5 ± 3.4
Cys6(O)	**–**	**WAT1/Nε2**	**–**	**Asp76(Oδ1)**	**97.3 ± 1.4**	**104.5 ± 2.3**	**94.2 ± 6.0**	**98.2 ± 3.7**
Cys6(O)	–	WAT1/Nε2	–	Thr91(Oγ1)	102.7 ± 2.2	102.1 ± 1.6	94.7 ± 3.5	99.6 ± 5.0
Cys6(O)	**–**	**WAT1/Nε2**	**–**	**Thr/Gln93(Oγ1/Cδ)**	**119.9 ± 18.6**	**123.9 ± 2.6**	—	**104.0 ± 2.7**
Asp76(Oδ1)	–	WAT1/Nε2	–	Thr91(Oγ1)	51.6 ± 1.7	50.0 ± 1.4	47.0 ± 1.7	46.7 ± 2.8
Asp76(Oδ1)	**–**	**WAT1/Nε2**	**–**	**Thr/Gln93(Oγ1/Cδ)**	**111.5 ± 10.1**	**103.0 ± 2.7**	—	**137.8 ± 4.9**
Thr91(Oγ1)	–	WAT1/Nε2	–	Thr/Gln93(Oγ1/Cδ)	61.5 ± 9.4	63.1 ± 2.3	—	94.5 ± 3.8

[a] In case of Thr93Gln RNase T1, the equivalent atoms Gln93(Nε2) and Gln93(Cδ) have been considered.
[b] Average value calculated from four molecules in one asymmetric unit.
[c] Closest donor/acceptor sites are marked in bold characters.

Table 4. *The average B-factor of WAT1 and Nϵ2, their potential hydrogen donor/acceptor partners, and the whole protein molecule (Å^2)*

	Wild-type[a]	Asn9Ala[a]	Thr93Ala[a]	Thr93Gln[a]
WAT1/Nϵ2	18.8 ± 4.7	18.7 ± 5.4	28.6 ± 6.2	20.9 ± 3.5
Cys6(O)	16.1 ± 1.3	20.9 ± 3.7	19.7 ± 1.1	17.8 ± 2.7
Asn9(Nδ2)	18.7 ± 3.3	—	26.4 ± 3.1	24.1 ± 6.9
Asp76(Oδ1)	13.1 ± 2.2	12.5 ± 2.5	13.0 ± 1.1	13.9 ± 5.0
Thr91(Oγ1)	14.1 ± 0.6	15.1 ± 3.8	15.3 ± 0.4	14.4 ± 1.4
Thr93(Oγ1)	18.1 ± 2.3	17.7 ± 4.0	—	—
Protein molecule	18.7 ± 7.5	19.8 ± 8.7	20.4 ± 9.3	19.6± 8.9

[a]Average value calculated from four molecules in one asymmetric unit.

temperature and solvent viscosity), for RNase T1 (2.2 mM, pH* 5.5) deduced from ^{13}C relaxation rates (Engelke & Rüterjans, 1997). With $N_\alpha = 360$, estimated from the solvent accessible surface area of 5,400 Å^2 for RNase T1, we obtain $\rho = 6.8$, somewhat larger than the typical range of four to five found for most small proteins (Denisov & Halle, 1996). This indicates a high-frequency relaxation contribution from several water molecules with residence times in the nanosecond range, as indeed expected from the unusually large number of hydrated pockets and clefts on the surface of RNase T1 (Malin et al., 1991; Martinez-Oyanedel et al., 1991). The presence of such moderately long-lived water molecules (with τ_w of the same order as τ_R and therefore $\tau_\beta < \tau_R$) can explain the small but significant deviation from the Lorentzian fit at high frequencies seen in Figure 4A.

If the residence time of WAT1 is in the range 10^{-9}–10^{-6} s, we expect the dispersion step from the Thr93Gln mutant to be slightly smaller than that from wild-type RNase T1. Figure 4A shows that this is the case. If the residence time τ_w of WAT1 is much longer than τ_R, we can obtain the mean-square order parameter S^2 for WAT1 directly from the difference of the $N_\beta S^2$ parameters deduced from the two fits in Figure 4A (cf. Table 5). The NMRD data are sufficiently accurate, however, that we can analyze the differ-

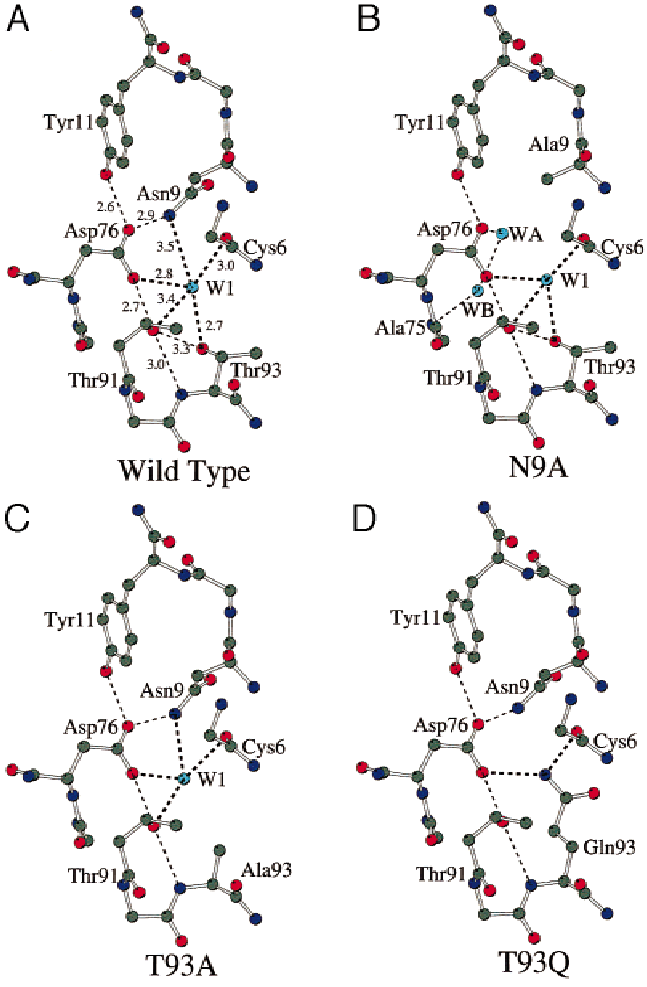

Fig. 3. Comparison of the local hydrogen bond networks around WAT1 in wild-type RNase T1 and three mutants. In each case, molecule A of the four molecules present in the asymmetric unit is shown. The local structures of the other three molecules (**B**, **C**, and **D**) in the asymmetric unit of the crystal are essentially identical. (**A**) Wild-type, all relevant interatomic distances are shown; (**B**) Asn9Ala; (**C**) Thr93Ala; (**D**) Thr93Gln.

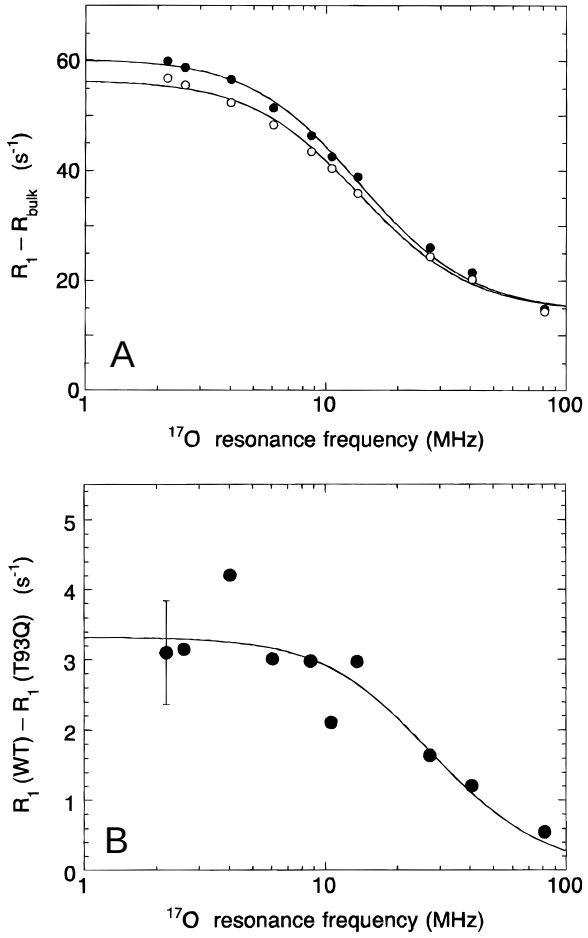

Fig. 4. A: Dispersion of the water ^{17}O longitudinal relaxation rate R_1 in aqueous solutions (HDO, pH* 4.9, 27 °C) of wild-type RNase T1 (closed circle) and the Thr93Gln mutant (open circle), both at 2.14 mM. The curves resulted from three-parameter fits with a Lorentzian spectral density function. The estimated error bars are of the same size as the data symbols. **B:** Direct two-parameter fit to the difference of the ^{17}O relaxation data (shown in Fig. 4A) from wild-type RNase T1 and the Thr93Gln mutant. The estimated error is indicated for one data point.

Table 5. *Parameters derived from ^{17}O and ^{2}H NMRD data*[a]

Protein	Nucleus	τ_β (ns)	$N_\beta S^2$	$N_\alpha \rho$ (10^3)
Wild-type	^{17}O	6.4 ± 0.3	3.1 ± 0.2	2.5 ± 0.1
Thr93Gln	^{17}O	6.6 ± 0.3	2.8 ± 0.2	2.4 ± 0.1
Difference	^{17}O	3.3 ± 0.7	0.45 ± 0.08	—
Wild-type	^{2}H	6.2 ± 0.4	5.9 ± 0.4	2.3 ± 0.3
Thr93Gln	^{2}H	6.5 ± 0.4	5.4 ± 0.3	2.5 ± 0.2
Difference	^{2}H	3.3[b]	0.39 ± 0.09	—

[a] Parameter errors estimated from Levenberg–Marquardt fits with reduced chi-square ≈ 1.0.
[b] Parameter value frozen in the fit.

ence data directly without making any assumptions about the residence time of WAT1. A direct two-parameter fit to the difference NMRD data (Fig. 4B) yields $\tau_\beta = 3.3 \pm 0.7$ ns and $S^2 = 0.45 \pm 0.08$. With $\tau_R = 6.5 \pm 0.3$ ns, we thus obtain a residence time of $\tau_w = 7 \pm 3$ ns for WAT1 at 27 °C. This is essentially the same as the residence time of 8 ± 1 ns (also at 27 °C) for three to six water molecules residing in surface pockets of RNase A (Denisov & Halle, 1998). The present result, however, is the first determination of the residence time of an individual water molecule at an identified hydration site at the surface of a protein. A similar difference NMRD experiment involving the Ser36Gly mutant of BPTI has previously provided the residence time (170 ± 20 μs at 27 °C) of a deeply buried water molecule (Denisov et al., 1996).

The order parameter S^2 reflects the degree of orientational averaging by rotational motion of the water molecule relative to the protein on time scales shorter than τ_β (3 ns). S^2 ranges from 0 for a spherically disordered water molecule to 1 for a rigidly bound water molecule. For the deeply buried water molecule W122 in BPTI, $S^2 = 0.89 \pm 0.08$ (Denisov et al., 1997). This water molecule makes four hydrogen bonds to the backbone in a nearly tetrahedral geometry. The value, $S^2 = 0.45 \pm 0.08$, found here for WAT1 in RNase T1 coincides with the value, $S^2 = 0.45 \pm 0.02$, obtained (as an average) for three buried water molecules in the Tyr35Glu mutant of BPTI (Denisov et al., 1997). Like WAT1 in RNase T1, these water molecules make three or four strong (2.7–3.1 Å) hydrogen bonds to the protein. It is not possible, from the ^{17}O order parameter alone, to identify the motions responsible for the orientational averaging. Within a harmonic libration model, however, $S^2 = 0.45$ corresponds to an RMS libration angle of ca. 25° for motion around the water dipole axis (Halle et al., 1998). (Motions around the two perpendicular axes are much less effective in reducing S^2, and a symmetric 180° jump does not affect S^2 at all.)

The ^{17}O dispersion from the Thr93Gln mutant (Fig. 4A) must be due to long-lived water molecules (with τ_w in the range 10^{-9}–10^{-6} s) other than WAT1. The dispersion amplitude, yielding $N_\beta S^2 = 2.8 \pm 0.2$ (cf. Table 5), implies that there are at least three such water molecules and probably more (because S^2 is expected to be significantly less than 1). These water molecules, in addition to WAT1, are also responsible for the wild-type dispersion (Fig. 4A). As in RNase A, there are no completely buried water molecules in RNase T1. However, we identified a number of water molecules that were conserved in the different crystal structures of RNases T1 as well as in the crystal structures of a number of evolutionary related ribonucleases (see above). These water molecules, which include WAT1, are characterized by small accessibility to external solvent, low thermal *B*-factors, and several hydrogen bonds to protein atoms, factors that are indicative of a long residence time (Denisov & Halle, 1996). Taken together with the results presented in a recent NOE study (Pfeiffer et al., 1998), it is safe to conclude that the remaining water molecules responsible for the ^{17}O dispersion curve of the Thr93Gln mutant correspond to some of these conserved waters. Because the NMRD measurements were done in the absence of any competitive inhibitor, two water molecules, buried under the Tyr45 ring and identified in the 1.5 Å crystal structure of inhibitor-free wild-type RNase T1 as W129 and W204 (Martinez-Oyanedel et al., 1991), may also contribute to the ^{17}O dispersion curves. The contribution from these water molecules (W2, W3, W4, W6, W129, and W204) to the dispersion amplitude is expected to be reduced by orientational disorder ($S^2 < 1$) and, possibly, by residence times comparable to τ_R (as for WAT1).

The ^{2}H dispersions from wild-type RNase T1 and the Thr93Gln mutant (data not shown) are qualitatively similar to the ^{17}O dispersions in Figure 4A. The parameter values resulting from fits to the ^{2}H data are included in Table 5. The correlation time τ_β and the surface hydration parameter $N_\alpha \rho$ do not differ significantly from the corresponding ^{17}O results and are the same for the wild-type and mutant proteins (as for ^{17}O). The dispersion amplitude parameter, however, is twice as large for ^{2}H: $N_\beta S^2 = 5.9 \pm 0.4$ compared to 3.1 ± 0.2 for ^{17}O (wild-type). This difference is due to a contribution from rapidly exchanging labile hydrogens to the ^{2}H dispersion (Denisov & Halle, 1995a). At the experimental pH* value of 4.9, the labile hydrogen contribution is strongly dominated by carboxyl groups of which there are 13 in RNase T1, some of which are in the acidic form at this pH. If some of the long-lived water molecules undergo symmetric 180° flips on a sub-nanosecond time scale, we expect that $S^2(^2H) < S^2(^{17}O)$ (Halle et al., 1998). The water contribution to $N_\beta S^2(^2H)$ will then be less than 3.1. It is likely, therefore, that long-lived water molecules account for less than half of the ^{2}H dispersion at pH* 4.9. Although the ^{2}H dispersion amplitude is significantly larger for wild-type RNase T1 than for the Thr93Gln mutant, the larger scatter in the ^{2}H data precludes a direct difference fit (as done for ^{17}O in Fig. 4B). If the correlation time is taken from the ^{17}O difference fit ($\tau_\beta = 3.3$ ns), however, we obtain $S^2 = 0.39 \pm 0.09$ for WAT1, in agreement with the ^{17}O result. The replaced Thr93 hydroxyl hydrogen exchanges too slowly to contribute to ^{2}H relaxation and, therefore, does not affect the difference fit.

A functional role for the hydrogen bond network?

Several of the structurally conserved water molecules that we identified in RNase T1 are bound to amino acids adjacent in sequence to the active site residues His40, Glu58, Arg77, and His92 (WAT1, WAT6, WAT8, and WAT10). These waters may therefore affect the configuration of the amino acids required for catalysis (Malin et al., 1991) as well as the dynamics of the active site during the catalytic cycle. To test for a possible functional role of the hydrogen bond network involving WAT1, we analyzed the effect of the Asn9Ala, Thr93Ala, and Thr93Gln mutations on the enzymatic activity of RNase T1. We measured the conversion of guanyl(3′-5′)cytidine (GpC) to guanosine cyclic 2′,3′-phosphate (cGMP) and cytosine spectrophotometrically at 280 nm (Osterman & Walz, 1978). Initial rate experiments at GpC concentration ranging from 20 to 600 mM led to a hyperbolic plot of catalytic rate versus

Table 6. *Steady-state kinetics for the transesterification of GpC*

Enzyme	k_{cat} (s^{-1})	K_m (μM)	k_{cat}/K_m (s^{-1} μM^{-1})
Wild-type	348 ± 12[a]	216 ± 29[a]	1.61 ± 0.22[a]
Asn9Ala	226 ± 38	92 ± 45	2.46 ± 1.27
Thr91Ala	16 ± 1	79 ± 10	2.00 ± 0.27
Thr93Ala	81 ± 6	49 ± 11	1.65 ± 0.39
Thr93Gln	88 ± 9	43 ± 14	2.06 ± 0.70

[a]From Steyaert et al. (1994).

substrate concentrations, indicating that RNase T1 follows saturation kinetics for the transesterification reaction. The steady-state kinetic parameters k_{cat} and K_m are shown in Table 6. All the mutations reduce the turnover number as well as the Michaelis–Menten constant of RNase T1 for GpC. As wild-type RNase T1 follows diffusion-controlled Briggs–Haldane kinetics for this substrate ($K_m > K_s = 33$ μM; Steyaert et al., 1991), we conclude that the mutations reduce the chemical turnover of the substrate (k_{cat}) rather than its binding (K_s). It appears from our kinetic data that changes in the hydrogen bond network involving WAT1 affect the catalytic function of the protein. These changes are not due to a structural distortion of the active site, as we do not observe significant structural differences in the active sites of wild-type, Asn9Ala, Thr93Ala, and Thr93Gln RNase T1 in complex with the competitive inhibitor guanosine 2′-phosphate (2′-GMP, data not shown). Possibly, mutations at positions 91 and 93 indirectly affect the catalytic efficiency of the adjacent general acid His92 (Fig. 5) (Steyaert et al., 1990). His92 participates in a dynamic loop segment from residue 91 to 101 (Koellner et al., 1992). The pK_a of the catalytic histidine depends on the conformation of this loop (De Vos et al., 1998). Hydrogen bond networks involving waters may hide dynamic features that are a requisite for catalysis. Internal motions including dihedral angle fluctuations of the backbone, side-chain rotations, loop movements, and the dynamics of secondary structure elements or whole domains are indeed relevant to protein function and enzyme catalysis (Creighton, 1993).

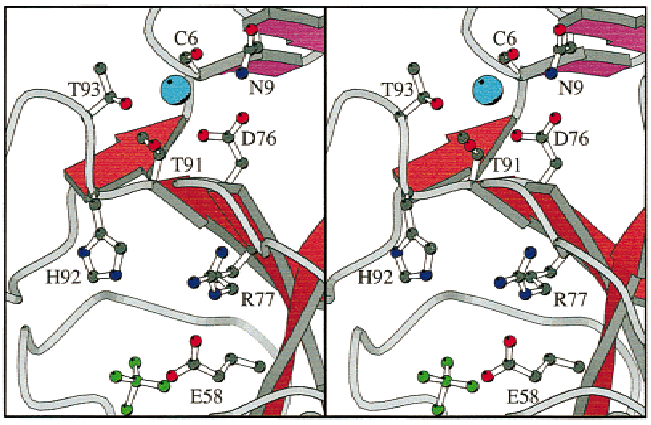

Fig. 5. Ribbon drawing showing the position of the hydration site relative to the active site. Secondary structure elements are colored as in Fig. 1. WAT1 is presented as a light blue sphere. Ligands of WAT1 (Asn9, Cys6, Asp76, Thr91, Thr93) as well as three adjacent active site residues (Gln58, Arg77, His92) are drawn in ball-and-stick representation. The phosphate group of the bound inhibitor 2′GMP is shown in green.

Conclusions

In the past, several investigators have focused on completely buried waters. We completed the first detailed biophysical characterization of an individual water on the surface of a protein. In the present work, we investigated the structural and functional role of a water site that is conserved not only in the different crystal structures of a particular protein, but also in a number of homologous proteins.

WAT1 of RNase T1 provides a unique opportunity to study water–protein interactions by protein engineering, because most of its hydrogen bonding partners involve side-chain atoms, allowing the use of site-directed mutagenesis to study its properties. The position of WAT1 is resistant to the deletion of the contacting side chains of Asn9 and Thr93. The relatively short residence time of WAT1 (7 ns) shows that this hydration site is frequently rearranged. The relatively small orientational order parameter ($S^2 = 0.45$) implies substantial rotational averaging on a sub-nanosecond time scale. The capacity of WAT1 to form four hydrogen bonds (low enthalpy) combined with its orientational disorder (high rotational entropy) may explain why evolution has preserved a water molecule rather than a side-chain atom at the center of the hydrogen bond network involving Cys6, Asn9, Asp76, Thr91, and Thr93. The effects of mutations around WAT1 on the kinetic parameters of RNase T1 are small but significant and probably relate to the dynamics of the active site.

Materials and methods

Identification of conserved water molecules

For two structures that are compared, water molecules are first identified that are closer than 5.0 Å to the nearest protein atom, taking into account the symmetry elements of the crystals. After superposition of the relevant portions of the two crystal structures, a hydration site was considered conserved between the two structures if both water molecules were found to be closer to each other than a predefined distance of 1 Å. All comparisons were done relative to the reference structure 1rga (Zegers et al., 1994). Additional test calculations using different reference structures yielded essentially identical results and are, therefore, not presented. Accessible surface areas were calculated using NACCESS according the method of Lee and Richards, using a probe sphere with radius 1.4 Å (Lee & Richards, 1971).

Oligonucleotide-directed mutagenesis, enzyme purification, and kinetic procedures

Overproduction and purification of wild-type RNase T1 have been described previously (Steyaert et al., 1990). The Asn9Ala, Thr93Ala, and Thr93Gln mutants were constructed with a PCR-based site-directed mutagenesis technique (Chen & Przybyla, 1994). The correct sequence of the complete gene was verified by DNA sequencing. Enzymes were purified to homogeneity as described (Mayr & Schmid, 1993), and their molecular weights were confirmed by mass spectrometry.

All kinetic experiments were performed at 35 °C in buffers containing 50 mM imidazole (pH 6.0), 50 mM NaCl (ionic strength = 0.1 M), and 2.5 mM EDTA. RNase T1 concentrations are based on $A_{278\,nm} = 1.54$ for a 0.1% solution (Shirley & Laurents, 1990). The steady-state kinetic parameters for the conversion of GpC to cGMP and C were determined from initial velocities by measuring the increase in absorbance at 280 nm (Zabinski & Walz, 1976) as described (Steyaert et al., 1991). The values and standard errors of the kinetic parameters were obtained from non-linear least-squares analysis using ORIGIN data analysis software (Microcal Systems, Northhampton, California).

Crystallization and data collection and structure determination

Conditions used to grow isomorphous crystals of wild-type, Asn9Ala, Thr93Ala, and Thr93Gln RNase T1 are given in Table 1. Data were collected using a MAR Image Plate detector and a RIGAKU rotating anode X-ray generator operated at 40 kV, 90 mA. The data were integrated using DENZO and subsequently scaled and merged using SCALEPACK (Otwinowski & Minor, 1997). The CCP4 program TRUNCATE (CCP4, 1994) was used to convert Is into Fs. The statistics of the data collections are summarized in Table 1.

The structure of the Thr93Ala mutant (the first for which X-ray data became available) was solved by molecular replacement using the program AMORE (Navaza, 1994). PDB entry 1rga (Zegers et al., 1994) was used as starting model. The isomorphous structures of the other mutants (Thr93Gln and Asn9Ala) and the wild-type protein were solved starting from the refined coordinates of the Thr93Ala structure. Refinement was done with X-PLOR version 3.851 (Brünger, 1992) using all reflections in the resolution range 10.0–2.05 Å. In each case, the refinement was started with a slow-cool stage to reduce bias toward the starting model. A bulk solvent correction was calculated after each rebuilding session. Water molecules were included (1) if they could be identified as peaks of at least 3σ in $F_o - F_c$ maps, (2) if they reappeared after refinement in $2F_o - F_c$ maps of at least 1σ, (3) if they made at least one reasonable hydrogen bond to a protein or inhibitor atom, and (4) if they showed no van der Waals clashes with any protein or inhibitor atom or with a previously identified water molecule. The quality of all refined structures was verified with PROCHECK (Laskowski et al., 1993) and is given in Table 1. Coordinates have been deposited in the Brookhaven Protein Data Bank (Bernstein et al., 1977) with accession codes 1bvi, 2hoh, 3hoh, and 4hoh.

NMRD measurements

For the NMRD measurements, wild-type and Thr93Gln RNase T1, purified as noted above, were dissolved in a 50:50% w/w mixture of H_2O enriched to 35 atom% ^{17}O and D_2O (both from Cambridge Isotope Laboratories, Andover, Massachusetts). No buffer was used. The measured pH* (uncorrected for isotope effects) was 4.9. Clear solutions were obtained after centrifugation for 5 min at 13,000 rpm. Protein concentrations were determined by complete amino acid analysis, yielding for both NMRD samples 2.14 mM (with an accuracy better than ±0.04 mM), corresponding to a water/protein mole ratio, $N_T = 25{,}400$. It was thus not necessary to apply any concentration correction in the difference NMRD analysis.

Oxygen-17 and deuteron longitudinal relaxation rates R_1 were measured as described (Denisov & Halle, 1995a, 1995b) at 10 magnetic fields in the range 0.38–14.1 T, using five conventional NMR spectrometers with fixed-field cryomagnets and a custom-built spectrometer with a field-variable iron magnet. The sample temperature was maintained at 27.0 °C. The relaxation rates of a bulk water reference sample (with the same solvent isotope composition as in the protein solutions) were $R_{bulk} = 150.6\ s^{-1}$ (^{17}O) and $2.01\ s^{-1}$ (^2H). The frequency dependence (dispersion) of the relaxation rate was analyzed in the usual way (Denisov & Halle, 1996; Halle et al., 1998).

Acknowledgments

This work was supported by the Vlaams Interuniversitair instituut voor Biotechnologie (VIB) and the Fonds voor Wetenschappelijk Onderzoek (FWO) Vlaanderen. We wish to thank Elke Brosens for technical assistance. We are grateful to Kazuo Nakamura, Jozef Sevcik, Guy Dodson, Yves Mauguen, Konstantin Panov, and Kostya Polyakov for generously supplying coordinates of crystal structures prior to publication and deposition. R. Loris and D. Maes are research associates of the FWO Vlaanderen.

References

Baker EN. 1995. Solvent interactions with proteins as revealed by X-ray crystallographic studies. In: Gregory RB, ed. *Protein–solvent interactions*. New York: Marcel Dekker, Inc. pp 143–189.

Bernstein FC, Koetzle TF, Williams GJB, Meyer EF Jr, Bice MD, Rodgers JR, Kennard O, Shimanouchi T, Tasumi M. 1977. The Protein Data Bank: A computer-based archival file for macromolecular structures. *J Mol Biol 112*:535–542.

Brünger AT. 1992. *X-PLOR (version 3.1): A system for crystallography and NMR*. New Haven, Connecticut: Yale University.

CCP4. 1994. The CCP4 suite: Programs for crystallography. *Acta Crystallogr D 50*:760–763.

Chen B, Przybyla AE. 1994. An efficient site-directed mutagenesis method based on PCR. *Biotechniques 17*:657–659.

Creighton TE. 1993. *Proteins: Structure and molecular properties*. New York: W.H. Freeman and Company.

Denisov VP, Halle B. 1995a. Hydrogen exchange and protein hydration: The deuteron spin relaxation dispersions of bovine pancreatic trypsin inhibitor and ubiquitin. *J Mol Biol 245*:698–709.

Denisov VP, Halle B. 1995b. Protein hydration dynamics in aqueous solution: A comparison of bovine pancreatic trypsin inhibitor and ubiquitin by oxygen-17 spin relaxation dispersion. *J Mol Biol 245*:682–697.

Denisov VP, Halle B. 1996. Protein hydration dynamics in aqueous solution. *Faraday Discuss 103*:227–244.

Denisov VP, Halle B. 1998. Thermal denaturation of ribonuclease A characterized by water ^{17}O and ^2H magnetic relaxation dispersion. *Biochemistry 37*:9595–9604.

Denisov VP, Peters J, Hörlein HD, Halle B. 1996. Using buried water molecules to explore the energy landscape of proteins. *Nat Struct Biol 3*:505–509.

Denisov VP, Venu K, Peters J, Hörlein HD, Halle B. 1997. Orientational disorder and entropy of water in protein cavities. *J Phys Chem B 101*:9380–9389.

De Vos S, Doumen J, Langhorst U, Steyaert J. 1998. Dissecting histidine interactions of ribonuclease T1 with asparagine and glutamine replacements: Analysis of double mutant cycles at one position. *J Mol Biol 275*:651–661.

Engelke J, Rüterjans H. 1997. Backbone dynamics of proteins derived from carbonyl carbon relaxation times at 500, 600 and 800 MHz: Application to ribonuclease T1. *J Biomol NMR 9*:63–78.

Esnouf R. 1997. An extensively modified version of Molscript that includes greatly enhanced coloring capabilities. *J Mol Graph Model 15*:132–143.

Halle B, Denisov VP, Venu K. 1998. Multinuclear relaxation dispersion studies of protein hydration. In: Berliner LJ, Krishna NR, eds. *Modern techniques in protein NMR*, vol 17. New York: Plenum.

Koellner G, Choe H-W, Heinemann U, Grunert H-P, Zouni A, Hahn U, Saenger W. 1992. His92Ala mutation in ribonuclease T1 induces segmental flexibility. *J Mol Biol 224*:701–713.

Laskowski RA, MacArthur MW, Moss DS, Thornton JM. 1993. Procheck: A program to check the stereochemical quality of protein structures. *J Appl Crystallogr 26*:283–291.

Lee B, Richards FM. 1971. The interpretation of protein structures: Estimation of static accessibility. *J Mol Biol 55*:379–400.

Malin R, Zielenkiewicz P, Saenger W. 1991. Structurally conserved water molecules in ribonuclease T1. *J Biol Chem 266*:4848–4852.

Martinez-Oyanedel J, Choe H-W, Heinemann U, Saenger W. 1991. Ribonuclease T1 with free recognition and catalytic site: Crystal structure analysis at 1.5 Å resolution. *J Mol Biol 222*:335–352.

Mayr LM, Schmid FX. 1993. A purification method for labile variants of ribonuclease T1. *Protein Exp Purif 4*:52–58.

Meyer E. 1992. Internal water molecules and H-bonding in biological macromolecules: A review of structural features with functional implications. *Protein Sci 1*:1543–1562.

Navaza J. 1994. AMoRe: An automated package for molecular replacement. *Acta Crystallogr A 50*:157–163.

Osterman HL, Walz FG. 1978. Subsites and catalytic mechanism of ribonuclease T1: Kinetic studies using GpA, GpC, GpG, and GpU as substrates. *Biochemistry 17*:4124–4130.

Otwinowski Z, Minor W. 1997. Processing of X-ray data collected in oscillation mode. *Methods Enzymol 276*:307–326.

Pfeiffer S, Spitzner N, Löhr F, Rüterjans H. 1998. Hydration water molecules of nucleotide-free RNase T1 studied by NMR spectroscopy in solution. *J Biomol NMR 11*:1–15.

Shirley BA, Laurents DV. 1990. Purification of recombinant ribonuclease T1 expressed in *Escherichia coli*. *J Biochem Biophys Methods 20*:181–188.

Steyaert J, Haikal AF, Wyns L. 1994. Investigation of the functional interplay between the primary site and the subsite of RNase T1: Kinetic analysis of single and multiple mutants for modified substrates. *Proteins Struct Funct Genet 18*:318–323.

Steyaert J, Haikal AF, Wyns L, Stanssens P. 1991. Subsite interactions of ribonuclease T1: Asn36 and Asn98 accelerate GpN transesterification through interactions with the leaving nucleoside N. *Biochemistry 30*:8666–8670.

Steyaert J, Hallenga K, Wyns L, Stanssens P. 1990. Histidine-40 of ribonuclease T1 acts as base catalyst when the true catalytic base, glutamic acid-58, is replaced by alanine. *Biochemistry 29*:9064–9072.

Zabinski M, Walz FG. 1976. Subsites and catalytic mechanism of ribonuclease T1: Kinetic studies using GpC and GpU as substrates. *Arch Biochem Biophys 175*:558–564.

Zegers I, Haikal AF, Palmer R, Wyns L. 1994. Crystal structure of RNase T1 with 3′-guanylic acid and guanosine. *J Biol Chem 269*:127–133.